Anterior cingulate is a source of valence-specific information about value and uncertainty

Ilya E. Monosov (1)

(1) Department of Neuroscience, Washington University, School of Medicine, 660 S. Euclid Avenue, St. Louis, MO 63110

Correspondence should be addressed to Dr. Ilya E. Monosov at ilya.monosov@gmail.com

Author contributions: I.E.M designed the research, performed the research, analyzed the data, and wrote the paper.

The author declares no conflict of interest.

Acknowledgements

This work was supported by the Defense Advanced Research Projects Agency (DARPA) Biological Technologies Office (BTO) ElectRx program under the auspices of Dr. Doug Weber through the CMO Grant/Contract No.HR0011-16-2-0022. I am grateful to Ms. Ying Jiang for assisting in data acquisition, to Ms. Kim Kocher for fantastic animal care and training, to Ms. Katherine Conen, Mr. J. Kael White, Mr. Ben Acland, and Mr. Mike Traner for reading earlier versions of this manuscript.

<Summary>

Expectations of rewards and punishments can promote similar behavioral states, such as vigilance, and distinct behavioral states, such as approach or avoidance. However, the cortical circuits that underlie this behavioral diversity are poorly understood. I show that many anterior-cingulate (ACC) neurons represent expected value and uncertainty in a valence-specific manner, about either rewards or punishments. This flexibility may facilitate the top-down control of many reward- and punishment-related behaviors.

<Introduction>

Actions to maximize rewards and minimize threats or punishments are thought to be controlled by a region of the prefrontal cortex (PFC) called the anterior cingulate cortex (ACC). But how this control is accomplished is unclear. Generally, there are several views of how ACC controls motivated behavior (1-9). The first posits that the ACC neurons rank-order outcomes (such as rewards and punishments) by their utility or value. This "signed" value signal is then read-out from ACC by other brain areas to guide action towards the best possible option or outcome (2, 5-8, 10). A second theory posits that ACC controls negative-affect, threat, and pain driven behaviors. This theory suggests that many ACC neurons ought to display a preference for punishment-related information (11-14). A third theory suggests that the ACC is primarily engaged in deploying attention to monitor task-performance and detect errors in our predictions and actions (15-22). This theory predicts that many ACC neurons ought to be activated by salient, engaging, and cognitively demanding situations, irrespective of their valence. Finally, a fourth theory, based on recent imaging studies, identifies ACC as a central hub for processing information about uncertainty and other exploration- and learning-related variables, such as the value of foraging (23-27). Several views suggest that ACC could support some or even many of these functions (1, 3, 4, 6, 7, 22, 27-32). However, to date, it remains unclear how it would do so. One difficulty in reconciling these theories is that it is not known whether the same ACC neurons represent the value and uncertainty of predictions about rewards and punishments.

Here I recorded single neuron activity from macaque ACC while monkeys experienced predictions about rewards and punishments. The resulting data indicate that the ACC contains distinct groups of neurons that process appetitive, aversive, salient, and uncertain information. Overall, the data caution against a unified view of ACC and suggest that the ACC may contain circuits that contribute to the top-down control of a wide-range of behaviors in distinct but complementary ways.

<Results>

To test how single ACC neurons signal information about reward, punishment, and uncertainty, I conditioned two monkeys with an appetitive-aversive behavioral procedure that contained two separate contexts, or *blocks.* One block contained 12 trials in which three visual fractal objects (conditioned stimuli, CS) predicted rewards (juice) with 100, 50, and 0 % chance. The second block contained 12 trials in which three visual fractal CSs predicted punishments (air puffs) with 100, 50, and 0 % chance (Figure 1A). The

monkeys did not have to fixate the CSs to complete the trial (Methods). The design was such that, 100% reward CS theoretically had the highest value in the reward block, and 0% punishment CS had the highest value in the aversive-block. Hypothetical encoding strategies of reward and punishment predictions are shown in Figure 1B (value exclusively for punishment- or reward-associated CSs, green and blue line, but not both; general value for both punishment- and reward-associated CSs, purple line; predicted intensity of outcome regardless of whether it's a reward or punishment, red line).

As in our previous studies (33, 34), after > 1 month of training, the monkeys understood the behavioral procedure. Their CS-related anticipatory mouth movements (e.g., licking of the juice spout) and anticipatory blinking were correlated to the probability of reward and punishment (Spearman's rank correlations; $p<0.01$), respectively. While these anticipatory responses were related to the expected value of the CSs, other behaviors, such as gaze, were driven by the absolute expected value of the CSs (often called motivational intensity or salience (35)) and by outcome uncertainty. Particularly, the monkeys' gaze was initially drawn to the CSs associated with the most probable outcome (100 % CSs), irrespective of valence (Figure 1C - left). Later in the trial, in the reward block, the monkeys' gaze was most strongly attracted towards the 50% reward CS (Figure 1C – middle; rank sum test; $p<0.01$). We could not reliably observe CS-related gaze behavior during the last second of the punishment-predicting CSs because the gaze signal was quenched by defensive blinking (Figure 1C - right).

To study punishment, it is crucial to verify that the outcome or unconditioned stimulus is aversive. It could be that blinking behaviors in Figure 1C reflect conditioning, but not aversion. To address this issue, we utilized distinct reward and punishment blocks that contained abort cues during ~50% of the trials (Methods). If the monkeys made a saccade to the abort cue, the trial was aborted (Figure 1D). Because these reward- and punishment- blocks alternate, the optimal reward-driven strategy would be to rapidly abort every trial in which the 100% and 50% reward CSs were not presented. In contrast, the monkeys' aborting behaviors were influenced by reward, punishment, and uncertainty. In the punishment block, monkeys actively aborted punishment-predicting CSs faster and more often than the 0% punishment CS, confirming that the air puff was an aversive outcome (Figure 1E). Also, monkeys aborted 50% reward CSs less than 100% reward CS trials (though, note that the proportion of aborted trials during either 100 or 50% reward CSs was extremely low). This decrease in abort-error rate is consistent with the observations in Figure 1C (middle) that the 50% reward CS captured attention (despite having a lower expected value than 100% reward CS), reducing the number of saccades to the location of the abort-cue.

In sum, the behavioral data suggest that monkeys utilized different representations (or encoding strategies) of rewards and punishments to influence their behaviors. Next, we asked if the ACC contains distinct representations of rewards and punishments or if ACC neurons encode rewards and punishments with a common currency, such as a general value signal (Figure 1B). The locations of ACC neuronal recordings are shown

in Supplemental Figure 1 and match the locations of neuronal recordings in previous studies of macaque ACC (5, 9, 32, 36, 37).

The neuronal recordings revealed (*1*) that many ACC neurons represent expected value in a valence-specific manner, signaling the probability of either rewards or punishments; and (*2*) also that many ACC neurons prefer uncertain CSs in a valence-specific manner, often displaying preference for either reward or punishment uncertainty.

First, to summarize the valence encoding strategies of ACC neurons, we performed correlation analyses for each recorded neuron (n=329) which assessed the relationship of CS-responses and outcome probability (Methods). The summary is shown in Table 1 and the correlation coefficients are shown in Supplemental Figure 2. Most neurons that displayed significant correlations with outcome probability (Spearman's rank correlation; $p<0.05$) did so in a valence specific manner, for either reward or punishment probability.

Valence-specific, n = 164 / 329 **49.9%**		**Valence non-specific**, n = 45 / 329 **14%**	
Reward value n = 92 / 329	**Punishment value** n = 72 / 329	**Intensity** n =32 / 329	**General Value** n = 13 / 329
Monkey 1, n=21/170 Monkey 2, n=71/159	Monkey 1, n=60/170 Monkey 2, n=12/159	Monkey 1, n=22/170 Monkey 2, n=10/159	Monkey 1, n=7/170 Monkey 2, n=6/159

Two valence-specific example neurons are shown in Figure 2A. The first neuron displayed greatest excitation to punishment-predicting CSs and did not differentiate amongst 100, 50, and 0% reward CSs. The second neuron displayed greatest excitation to reward-predicting CSs (strongest to 100% reward) and did not differentiate amongst 100, 50, and 0% punishment CSs.

Population analyses (Table 1) and a qualitative examination of neuronal responses (Figure 2A and Supplemental Figure 3) suggested that many ACC neurons signal value in a valence-specific manner. To study this observation on a population level in ACC, we analyzed the differences in neuronal responses for good outcomes and bad outcomes in the reward (x-axis in Figure 2B) and punishment (y-axis in Figure 2B) blocks. These analyses confirmed that most value coding neurons display valence-specific responses (blue and green colored data in Figure 2; Supplemental Figure 2-3). The second most common group of ACC neurons signaled the motivational intensity or unsigned value of the CSs (red in Figure 2). Few neurons showed a generalized value signal that rank-ordered the reward or punishment predictions according to their expected value (100>50>0% rewards and 0>50>100% punishments; purple dots in Figure 2).

Responses to the outcomes also tended to be valence specific. Many ACC neurons also selectively and distinctly signaled reward omissions, reward deliveries, punishment omissions, and punishment deliveries (Supplemental Figure 2). To summarize, the data thus far show that ACC can encode the values of predictions and deliveries of rewards and punishments in distinct population of neurons.

Next, we assess if and how single ACC neurons encode uncertainty. In contrast with the hypothesis that ACC encodes economic or general “common currency” values, some recent neuroimaging studies have highlighted the ACC as a central hub for processing outcome uncertainty and guiding behaviors aimed to reduce this uncertainty. However, single neuron evidence for uncertainty processing in ACC has been missing.

We found that 88 uncertainty selective neurons in the ACC (Methods), some of which responded selectively for punishment uncertainty. An example neuron is shown in Figure 3A (left). This neuron did not respond to reward predicting CSs or reward outcomes. In the punishment block, the neuron was most strongly activated by 50% punishment CS and this signal persisted until the trial outcome. Amongst uncertainty selective neurons, 23/88 neurons were selectively excited by punishment uncertainty but not reward uncertainty (Figure 3B; Supplemental Figure 4). 0 were selectively inhibited by punishment uncertainty (Figure 3D). Among the punishment-uncertainty neurons, 11 neurons displayed significant variability among the reward block CSs (Figure 3D – left; blue dots) but there was no obvious trend for positive or negative reward value coding amongst them. These results show that some ACC neurons signal punishment uncertainty in a selective manner, and that a minority of them can also multiplex this uncertainty signal with information about rewards.

Consistent with the observations that ACC signals task-related information in a valence specific manner (Figure 2), we also found neurons that preferred reward uncertainty but not punishment uncertainty (Figure 3B). An example neuron is shown in Figure 3A (right). This neuron responded to the 50% reward CS and maintained tonic firing until the time of the trial outcome (reward or no reward). It was not modulated by punishment predicting CSs. 45/88 uncertainty selective neurons were excited by reward uncertainty while 12/88 uncertainty selective neurons were inhibited. A 26/45 of reward uncertainty excited neurons also carried information about punishment probability; Figure 3B and Supplemental Figure 4). Among these, almost all were enhanced by increased probability of punishment (Figures 3C and 3E). Lastly, a minority of uncertainty selective neurons (8/88) were selective for both reward and punishment uncertainty (Figure 3B – inset). In sum, our findings show that ACC can signal uncertainty about either rewards or punishments in a valence-specific and selective manner or to multiplex information about uncertainty and value in multiple manners (Supplemental Figure 5).

Uncertainty can arise due to variability in outcomes or due to the possibility of making an error. For example, in our behavioral procedure aborting a reward associated CS is an error because it reduces the probability of reward on that trial to 0%. Though we observed few such errors (Figure 1), the anticipation of the abort cue resulted in increases of overt attention towards the reward-possible CSs and the activity of

uncertainty neurons in ACC, but not value coding ACC neurons (Supplemental Figure 6). Therefore, ACC uncertainty neurons are sensitive to uncertainty arising due to internal processing (that increases attention (27)) as well as due to uncertain stimulus-outcome associations.

<Discussion>

To obtain rewards and avoid punishments we must detect them, estimate their uncertainty, and track and predict their value. Here, the data show that the anterior cingulate (ACC) has the capacity to mediate these functions by specifically and distinctly signaling information about the value and uncertainty of rewards and punishments, and to multiplex them. The multiple valence coding strategies in ACC may support its roles in the control of value-based action (2, 3, 7, 8, 28, 36, 38) and of uncertainty-driven processes such as learning and monitoring, risk-seeking, and the identification of novel or uncertain environments (1, 4, 26, 27, 32).

The results are mostly inconsistent with several unified theories of ACC function. First, there was no indication that the majority of ACC neurons signaled aversive or noxious predictions or outcomes. Second, our data are inconsistent with the notion that many single ACC neurons encode a general value or common currency signal that generalizes across appetitive and aversive contexts. Specifically, very few ACC neurons displayed positive relationships with reward probability and negative relationships with punishment probability (or vice versa). Since rewards and punishments can promote similar behavioral states, such as vigilance, or distinct behavioral, states such as approach and avoidance, the heterogeneous valence-specific value signals in ACC may facilitate a more flexible capacity for control of a wide range of behavior (36). How valence specific value signals in ACC and valence nonspecific value signals in the amygdala (39, 40) and dopamine neurons (35) contribute to value-driven behaviors will be an important direction of our future studies.

This study is the first to demonstrate a selective punishment-uncertainty signal in the brain. Punishment uncertainty neurons were often found in more anterior and ventral regions of the bank of the ACC (Supplemental Figure 1) while reward uncertainty neurons were found in all areas, but were particularly common in the dorsal extent of the ACC. Since the dorsal and ventral regions of the dorsal ACC have distinct projection patterns to the striatum, amygdala, cortex, and brain stem (41-45), one possibility is that reward and punishment uncertainty are mediated by distinct circuits involving somewhat different (but overlapping) areas of ACC. This conjecture is further supported by a series of experiments in which we identified neurons in two anatomically distinct networks that selectively signal information about reward uncertainty, but not punishment uncertainty: the septal-basal forebrain network and the striatal-pallidal

network (33, 34, 46, 47). Both, of these networks receive inputs from, and send direct and indirect inputs to, the ACC, and neither contains neurons that signal punishment uncertainty.

The finding of a selective punishment uncertainty signal in the brain will provide new opportunities to study internal states such as anxiety and depression, which are thought to be strongly driven by persistent uncertainty about bad outcomes (25, 48-51). However, to move forward it will be crucial to identify precisely which brain regions receive and process punishment uncertainty signals from ACC and assess how the ACC interacts with the two reward-uncertainty selective networks to control reward uncertainty related action and internal states.

A recent neurophysiological study strongly suggests that ACC neurons display selectivity for contexts (or tasks) (52). It remains possible that valence specificity observed here reflects the context-specificity of value coding in ACC. However, we observed that the reward/punishment tuning of ACC value sensitive neurons did not change across blocks that contained active behavior to approach or avoid rewards and punishments, and blocks in which monkeys could not actively abort trials (abort-cues blocks versus no-abort cue blocks; Supplemental Figure 6). It may be that valence-specific value coding in ACC in this study indeed reflects the specificity in tuning of ACC neurons, but that may be mediated by context selectivity.

Identifying neuronal mechanisms that facilitate flexible control of action and learning toward rewards and away from punishments remains a central pursuit of systems neuroscience. Here, we demonstrate a remarkable diversity and valence-specificity of ACC neurons that may in part provide a neuronal substrate for such capacity. The data suggest that the ACC has multiple distinct and cooperative functions in behavioral control relative to reward, punishment, and their uncertainty.

Figure 1 - The reward-punishment behavioral procedure. (**A**) Monkeys experienced two types of distinct blocks of trials in which three visual fractal conditioned stimuli (CSs) predicted rewards and punishments with 100, 50, and 0% chance. The reward block consisted of 12 trials in which reward was possible, and the punishment block consisted of 12 trials in which punishment was possible. (**A-right**) Structure of a single trial. CS could appear in the center (as shown) or peripherally, 10 degrees to the left or right of center. (**B**) Theoretical valence coding strategies in the reward-punishment procedure. (**C**) Monkeys' behaviors were motivated by reward, punishment, and uncertainty. (**C-left**) Cumulative probability functions of peripheral-CS gaze acquisition time. In reward or punishment block, the speed of CS acquisition was correlated with outcome probability (Spearman's rank correlations; $p<0.01$). (**C-middle**) Proportion of trials the

monkeys oriented to the location of peripheral CSs shown across the entire CS epoch for reward- and punishment-block trials. During the last 1000 milliseconds of the trial the monkeys' gaze was preferentially attracted to the 50% reward CS ($p<0.01$; rank sum test). (**C-right**) Proportion of trials the monkeys blinked shown across the entire CS epoch for reward- and punishment-block trials. Insets show mean proportion of time monkeys blinked during the last 500 ms of the CS epoch. (**D**) In distinct blocks we included an abort cue during ~50% of the trials (Methods). Structure of trials with an abort cue. (**D-left**) – trials in which the monkeys did not abort (eye position is schematized by the red arrow); (**D-right**) – trials in which the monkeys aborted the trial. (**E**) Proportion of trials aborted in the reward block (top-left) and punishment block (top-right). The speed of trial aborting decreased with increasing punishment probability (bottom). The black-gray color legend for (**C and E**) is in (**A**). Error bars indicate standard error. Single asterisks indicate significance at a 0.05 threshold and double asterisks indicate significance at 0.01 threshold.

Figure 2 – Many anterior cingulate (ACC) neurons signal outcome probability in a valence-specific manner. (**A**) Two single ACC neurons, one that signals punishment probability (left) and one that signals reward probability (right). (**B**) Scatter plot shows the difference in CS responses for 100% and 0% CSs in the reward block (x-axis) versus difference in CS responses for 100% and 0% CSs in the punishment-block (y-axis). Green – neurons displayed significant differences between 100% and 0% CSs in the punishment block only, blue - neurons that displayed significant differences between 100% and 0% CSs in the reward block only, red – neurons that displayed significant differences between 100% and 0% CSs in both blocks and both differences were either positive or negative, and purple - neurons that displayed significant differences between 100% and 0% CSs in both blocks and the differences were of different sign. Colors in pie chart (inset) correspond to colors in scatter plot and in Figure 1B. (**B-right**) Single neuron responses (gray) shown separately for 4 major groups of outcome probability coding neurons in the scatter plot. Single neurons' CS responses were normalized to the maximum CS response; from 0 to 1. Uncertainty-selective neurons are studied separately in Figure 3.

Figure 3 - Distinct coding of reward and punishment uncertainty by many single ACC neurons. (**A**) Two single ACC neurons, one that signals punishment uncertainty (left) and one that signals reward uncertainty (right). (**B**) Single neuron discrimination indices of punishment and reward uncertainty selective neurons (top and bottom). Inset shows discrimination of 8 neurons that displayed uncertainty selectivity in both reward (x-axis) and punishment blocks (y-axis). Discrimination indices were obtained by ROC analyses (Methods). Values below 0.5 indicate selective suppression, indices above 0.5 indicate selective enhancement. (**C**) Punishment-uncertainty enhanced neurons in the reward block (left-scatter plot) and punishment block (right-scatter plot). Scatter plots show, for

individual neurons, the differences between 50% versus 100% CS responses (x-axis) and 50% versus 0% CS responses (y-axis). Red stars, Neurons showing significant differences in CS response in both 50–100% comparison and 50–0% comparison. Green stars, Neurons showing significant differences in only 50–0% comparison. Blue stars, Neurons showing significant differences in only 100–50% comparison. Black stars, neurons showing no significant differences. Single neuron and average CS responses (right) for two major groups of punishment uncertainty enhanced neurons (black and blue circles on the left). (**D**) Reward-uncertainty enhanced neurons. Conventions are the same as in (**C**).

Supplemental Figure 1 – Estimated locations of reward value, punishment value, reward uncertainty, and punishment uncertainty ACC neurons. The recording range was 6 to 17 mm from the center of the anterior commissure (AC), and also 3 neurons sampled 3 mm anterior to the AC were included in this study (which did not change any of the results). The anterior section on the left is 15 mm from the center of the AC and includes neurons recorded 17mm to 12 mm from the center of the AC. The posterior section on the right is 11 mm from the center of the AC, and includes the neurons sampled in the posterior extent of our recordings. It appears that different neuron types were mostly mixed within the ACC. One notable observation was the difference in the location of reward uncertainty and punishment uncertainty neurons. Punishment uncertainty neurons were found in the most anterior extent of our recordings and their locations were often within the ventral regions of the bank of the ACC, while reward uncertainty neurons were found widely throughout our recording area.

Supplemental Figure 2 - Coding of reward and punishments: CS responses and outcome prediction errors. (**A**) Correlation coefficients resulting in analyses for Table 1. Significance of each correlation was tested by 10,000 permutations ($p<0.05$; Methods). (**B**) Single neuron response differences between reward deliveries versus omissions following 50% reward CSs (x-axis) and differences between punishment deliveries versus omissions following 50% punishment CSs (y-axis). Significance was assessed by a Wilcoxon rank sum test ($p<0.05$). Colors in scatter plots and pie charts in **A-B** are the same as in Figure 2. (**C**) Counts of neurons displaying outcome PE coding (x-axis; determined from **B**) and CS sensitivity (y-axis; determined from **A**).

Supplemental Figure 3 – Neuronal activity of outcome probability value encoding neurons. Their activity in the reward (top) and punishment (bottom) blocks shown separately for 100, 50, and 0% CSs. Darkest traces show activity in 100% CS trials, lightest traces show activity in 0% CS trials (this is the same gray-black color scheme as in Figure 1). Dotted lines (after the outcome) represent outcome omissions. Shaded region represents standard error.

Supplemental Figure 4 – Neuronal activity of uncertainty selective neurons. Conventions are the same as in Supplemental Figure 3.

Supplemental Figure 5– ACC neurons uncertainty and value coding.

A visual summary of uncertainty and value sensitivity of all ACC neurons that displayed variance across the CSs (Kruskal Wallis test; $p<0.01$). Each neuron (shown as a row) contributes either an uncertainty or value discrimination index in each block. Matrix in this plot was organized by an unsupervised hierarchical clustering algorithm (Methods).

Supplemental Figure 6 – Behavioral and neuronal differences across blocks with and without abort cues. (**A**) Gaze behavior (left) and pupil dilation (right) is modulated by uncertainty and by abort possibility. Thick lines show behavior during blocks in which abort cues were never presented. Thin lines show behavior during blocks in which abort cues were presented 50 % of the time. Lines are colored as in Figure 1. Thick line at 750 ms following CS onset shows the time during which the abort cue would have been presented. Because the monkeys often aborted the non-rewarding trials and blinked during the later epochs of punishment-possible trials (Figure 1), we show behavior during 0% reward trials and 100, 50, and 0% punishment trials until the time of the abort cue would have been presented. After the time of the abort cue, we show behavior during trials in which monkeys did not abort. The possibility of abort cue presentation modulated gaze behavior ($p<0.01$; comparing reward-possible trials before the escape cues in abort-possible and no abort trials). In fact, monkeys could have looked away from the monitor to minimize the probability of error saccades after reward CSs were presented towards the abort cues. Instead, their overt attention increased towards reward CSs (100 and 50%). Pupil dilation (right) seemed to reflect gaze behavior (left), but with some lag. Both gaze and pupil dilation were affected by uncertainty (that was either due to the possibility of an abort cue during reward trials or by 50% reward predictions). (**B**) Neuronal activity before abort cues were presented (750 ms window following CS onset, before the abort cue) during blocks in which abort cues were never presented (blue) and may have been presented (green) for 6 groups of ACC CS modulated neurons. Consistent differences were observed for uncertainty-sensitive neurons following 100% reward CSs. Before averaging, single neurons' CS responses were normalized to the maximum CS response across 12 CS conditions; from 0 to 1. Error bars represent SEM. Ns – not significant (paired sigh rank test; $p>0.05$).

Online Methods

General procedures

Two adult male rhesus monkeys (*Macaca mulatta*) were used for the neurophysiology experiments (Monkeys B and Z). All procedures conformed to the Guide for the Care and Use of Laboratory Animals and were approved by the Washington University Institutional Animal Care and Use Committee. A plastic head holder and plastic recording chamber were fixed to the skull under general anesthesia and sterile surgical conditions. The chambers were tilted laterally by 35° and aimed at the anterior cingulate. After the monkeys recovered from surgery, they participated in the behavioral and neurophysiological experiments.

Data acquisition

While the monkeys participated in the behavioral procedure we recorded single neurons in the anterior cingulate. The recording sites were determined with 1 mm-spacing grid system and with the aid of MR images (3T) obtained along the direction of the recording chamber. This MRI-based estimation of neuron recording locations was aided by custom-built software (PyElectrode). Single-unit recording was performed using glass coated electrodes (Alpha Omega). The electrode was inserted into the brain through a stainless-steel guide tube and advanced by an oil-driven micromanipulator (MO-97A, Narishige). Signal acquisition (including amplification and filtering) was performed using Alpha Omega 44 kHz SNR system. Action potential waveforms were identified online by multiple time-amplitude windows with an additional template matching algorithm (Alpha-Omega). Neuronal recording was restricted to single neurons that were isolated online. Neuronal and behavioral analyses were conducted offline in Matlab (Mathworks, Natick, MA).

Eye position was obtained with an infrared video camera (Eyelink, SR Research). Behavioral events and visual stimuli were controlled by Matlab (Mathworks, Natick, MA) with Psychophysics Toolbox extensions. Juice, used as reward, was delivered with a solenoid delivery reward system (CRIST Instruments). Juice-related licking was measured and quantified using previously described methods (47). Airpuff (~35 psi) was delivered through a narrow tube placed 6–8 cm from the monkey's face.

Behavioral procedure

The reward-punishment behavioral procedure consisted of two alternating trial blocks: reward block and punishment block. In the reward block, three visual fractal conditioned stimuli (CS) were followed by a liquid reward (0.4 ml of juice) with 100%, 50%, and 0% chance, respectively. In the punishment block, three visual fractal CSs were followed by an air puff with 100%, 50%, and 0% chance, respectively. One block consisted of 12 trials with fixed proportions of trial types (each of the three CSs appears 4 times each block). The inter-trial-intervals (ITIs) ranged from ~2-6s.

Each trial started with the presentation of a trial-start cue at the center. The trial-start cue disappeared after 1 s and one of the three CSs was presented pseudo randomly (the CS could appear in three locations: 10 degrees to the left or to the right of the trial-start cue, or in the center). After 2.5 s, the CS disappeared, and the outcome (juice or aif puff or nothing) was delivered. The monkeys were not required to fixate.

Abort cues (Figure 1D) were presented during 50% of the trials in distinct blocks (abort-blocks) in one of three locations 10 degrees away from the CS. Abort blocks contained distinct visual fractals as CSs. Typically, a recording session contained the following repeating block structure: reward (abort) block, punishment (abort) block, reward block, punishment block, reward block, punishment block.

Data processing and statistics

Spike-density functions (SDFs) were generated by convolving spike-times with a Gaussian filter (σ = 100ms). All statistical tests were two-tailed. For comparisons between two task conditions for each neuron, we used a rank-sum test, unless otherwise noted. For comparisons between two task conditions across the population average we used a paired signed-rank test, unless otherwise noted. All correlation analyses were Spearman's rank correlations. The significance of the correlation analyses ($p<0.05$) was tested by 10,000 permutations (33, 34, 47, 53).

CS responses were measured in a single time window that started 100 ms from the CS onset until the outcome. Outcome responses were measured in a single 500 ms window that started 50 ms following outcome delivery. To normalize task-event related responses, we subtracted baseline activity (the last 500 milliseconds of the inter-trial interval) from the activity during the task-event related measurement epoch.

A neuron was defined as CS responsive if it displayed variance across CSs either in the reward or punishment block (Kruskal-Wallis test, $P < 0.01$). The statistical identification of uncertainty neurons was detailed previously (33, 34, 47, 53). As before, a neuron was defined as uncertainty sensitive if its CS responses varied across the 3 possible outcome predictions in either block (Kruskal-Wallis test, $P < 0.01$) and if its response to the uncertain CS (50%) was significantly stronger or weaker than its responses to both 100% and 0% CSs (two-tailed rank-sum test; $P < 0.05$; Bonferroni corrected). Therefore, a neuron could be uncertainty sensitive in reward block, punishment block, or both (Figure 3B).

To calculate receiver operating characteristic (ROC) that assessed neuronal discrimination of value and uncertainty, we compared spike counts during the CS epoch of two conditions. The analysis was structured so that area under curve (AUC) values > 0.5 indicate that the response for the value or uncertainty was a selective enhancement,

while values < 0.5 indicate that the response for the value or uncertainty was a selective suppression. In Figure 3B, ROC analyses were performed on uncertainty-selective neurons which compared 50 % CS responses with 100 % CS responses.

The goal of Supplemental Figure 5 was to visualize how uncertainty and value coding strategies co-occur in single neurons across the reward and punishment blocks. Each neuron was represented by a vector of 4 value and uncertainty discrimination indices ranging from 0 to 1. Value discrimination indices were obtained by ROC analyses that compared 100% and 0% CS responses. Uncertainty discrimination indices were obtained by ROC analyses that compared 50% and 100% CS responses. If a neuron did not pass the uncertainty sensitivity test (described above), the result of the ROC analysis was set to 0.5. If a neuron was uncertainty sensitive in one of the blocks, its value index was set to 0.5 in that block. Hierarchical clustering organized these data into 8 clusters. This was done by clustering on Euclidean distance utilizing Ward's minimum variance method. The number of clusters was approximated based on the results of expectation maximization algorithm (54). However, because clustering is a data mining method, here it is utilized to organize the matrix of neurons for qualitative observation. The results are interpreted as visual confirmation for multiple value and uncertainty coding strategies in ACC, not as evidence for discrete and stable clusters (e.g. robust to noise or increases or decreases in neuron number).

<References>

1. Heilbronner SR, Hayden BY. Dorsal Anterior Cingulate Cortex: A Bottom-Up View. Annual review of neuroscience. 2016.
2. Shenhav A, Botvinick MM, Cohen JD. The expected value of control: an integrative theory of anterior cingulate cortex function. Neuron. 2013;79(2):217-40. doi: 10.1016/j.neuron.2013.07.007. PubMed PMID: 23889930; PubMed Central PMCID: PMC3767969.
3. Shenhav A, Cohen JD, Botvinick MM. Dorsal anterior cingulate cortex and the value of control. Nature neuroscience. 2016;19(10):1286-91. doi: 10.1038/nn.4384. PubMed PMID: 27669989.
4. Kolling N, Wittmann MK, Behrens TE, Boorman ED, Mars RB, Rushworth MF. Value, search, persistence and model updating in anterior cingulate cortex. Nature neuroscience. 2016;19(10):1280-5. doi: 10.1038/nn.4382. PubMed PMID: 27669988.
5. Cai X, Padoa-Schioppa C. Neuronal encoding of subjective value in dorsal and ventral anterior cingulate cortex. The Journal of neuroscience : the official journal of the Society for Neuroscience. 2012;32(11):3791-808. Epub 2012/03/17. doi: 10.1523/JNEUROSCI.3864-11.2012. PubMed PMID: 22423100; PubMed Central PMCID: PMC3319456.
6. Wallis JD, Kennerley SW. Heterogeneous reward signals in prefrontal cortex. Current opinion in neurobiology. 2010;20(2):191-8.
7. Kennerley SW, Behrens TE, Wallis JD. Double dissociation of value computations in orbitofrontal and anterior cingulate neurons. Nature neuroscience. 2011;14(12):1581-9.
8. Rudebeck PH, Behrens TE, Kennerley SW, Baxter MG, Buckley MJ, Walton ME, Rushworth MF. Frontal cortex subregions play distinct roles in choices between actions and stimuli. The Journal of neuroscience : the official journal of the Society for Neuroscience. 2008;28(51):13775-85. doi: 10.1523/JNEUROSCI.3541-08.2008. PubMed PMID: 19091968.

9. Rudebeck PH, Bannerman DM, Rushworth MF. The contribution of distinct subregions of the ventromedial frontal cortex to emotion, social behavior, and decision making. Cognitive, affective & behavioral neuroscience. 2008;8(4):485-97. doi: 10.3758/CABN.8.4.485. PubMed PMID: 19033243.
10. Kennerley SW, Walton ME, Behrens TE, Buckley MJ, Rushworth MF. Optimal decision making and the anterior cingulate cortex. Nature neuroscience. 2006;9(7):940-7. doi: 10.1038/nn1724. PubMed PMID: 16783368.
11. Rainville P, Duncan GH, Price DD, Carrier B, Bushnell MC. Pain affect encoded in human anterior cingulate but not somatosensory cortex. Science. 1997;277(5328):968-71.
12. Wiech K, Tracey I. The influence of negative emotions on pain: behavioral effects and neural mechanisms. NeuroImage. 2009;47(3):987-94. Epub 2009/06/02. doi: 10.1016/j.neuroimage.2009.05.059. PubMed PMID: 19481610.
13. Iwata K, Kamo H, Ogawa A, Tsuboi Y, Noma N, Mitsuhashi Y, Taira M, Koshikawa N, Kitagawa J. Anterior cingulate cortical neuronal activity during perception of noxious thermal stimuli in monkeys. Journal of neurophysiology. 2005;94(3):1980-91.
14. Kwan CL, Crawley AP, Mikulis DJ, Davis KD. An fMRI study of the anterior cingulate cortex and surrounding medial wall activations evoked by noxious cutaneous heat and cold stimuli. Pain. 2000;85(3):359-74.
15. Hayden BY, Heilbronner SR, Pearson JM, Platt ML. Surprise signals in anterior cingulate cortex: neuronal encoding of unsigned reward prediction errors driving adjustment in behavior. The Journal of neuroscience : the official journal of the Society for Neuroscience. 2011;31(11):4178-87. Epub 2011/03/18. doi: 10.1523/JNEUROSCI.4652-10.2011. PubMed PMID: 21411658; PubMed Central PMCID: PMC3070460.
16. Ito S, Stuphorn V, Brown JW, Schall JD. Performance monitoring by the anterior cingulate cortex during saccade countermanding. Science. 2003;302(5642):120-2. Epub 2003/10/04. doi: 10.1126/science.1087847. PubMed PMID: 14526085.
17. Carter CS, Braver TS, Barch DM, Botvinick MM, Noll D, Cohen JD. Anterior cingulate cortex, error detection, and the online monitoring of performance. Science. 1998;280(5364):747-9.
18. Botvinick M, Nystrom LE, Fissell K, Carter CS, Cohen JD. Conflict monitoring versus selection-for-action in anterior cingulate cortex. Nature. 1999;402(6758):179-81. Epub 2000/01/26. doi: 10.1038/46035. PubMed PMID: 10647008.
19. van Veen V, Cohen JD, Botvinick MM, Stenger VA, Carter CS. Anterior cingulate cortex, conflict monitoring, and levels of processing. NeuroImage. 2001;14(6):1302-8. Epub 2001/11/15. doi: 10.1006/nimg.2001.0923. PubMed PMID: 11707086.
20. Botvinick MM, Braver TS, Barch DM, Carter CS, Cohen JD. Conflict monitoring and cognitive control. Psychological review. 2001;108(3):624-52. Epub 2001/08/08. PubMed PMID: 11488380.
21. Brown JW, Braver TS. Learned predictions of error likelihood in the anterior cingulate cortex. Science. 2005;307(5712):1118-21.
22. Ebitz RB, Platt ML. Neuronal activity in primate dorsal anterior cingulate cortex signals task conflict and predicts adjustments in pupil-linked arousal. Neuron. 2015;85(3):628-40. doi: 10.1016/j.neuron.2014.12.053. PubMed PMID: 25654259; PubMed Central PMCID: PMC4319115.
23. Kolling N, Behrens TE, Mars RB, Rushworth MF. Neural mechanisms of foraging. Science. 2012;336(6077):95-8. Epub 2012/04/12. doi: 10.1126/science.1216930. PubMed PMID: 22491854; PubMed Central PMCID: PMC3440844.
24. Behrens TE, Woolrich MW, Walton ME, Rushworth MF. Learning the value of information in an uncertain world. Nature neuroscience. 2007;10(9):1214-21. PubMed PMID: 17676057.
25. Hirsh JB, Mar RA, Peterson JB. Psychological entropy: a framework for understanding uncertainty-related anxiety. Psychological review. 2012;119(2):304-20. doi: 10.1037/a0026767. PubMed PMID: 22250757.

26. Burke CJ, Tobler PN. Reward skewness coding in the insula independent of probability and loss. Journal of neurophysiology. 2011;106(5):2415-22. doi: 10.1152/jn.00471.2011. PubMed PMID: 21849610; PubMed Central PMCID: PMC3214105.
27. Bryden DW, Johnson EE, Tobia SC, Kashtelyan V, Roesch MR. Attention for learning signals in anterior cingulate cortex. The Journal of neuroscience : the official journal of the Society for Neuroscience. 2011;31(50):18266-74. Epub 2011/12/16. doi: 10.1523/JNEUROSCI.4715-11.2011. PubMed PMID: 22171031; PubMed Central PMCID: PMC3285822.
28. Quilodran R, Rothe M, Procyk E. Behavioral shifts and action valuation in the anterior cingulate cortex. Neuron. 2008;57(2):314-25. doi: 10.1016/j.neuron.2007.11.031. PubMed PMID: 18215627.
29. Wallis JD, Rich EL. Challenges of Interpreting Frontal Neurons during Value-Based Decision-Making. Frontiers in neuroscience. 2011;5:124. doi: 10.3389/fnins.2011.00124. PubMed PMID: 22125508; PubMed Central PMCID: PMC3222102.
30. Wittmann MK, Kolling N, Akaishi R, Chau BK, Brown JW, Nelissen N, Rushworth MF. Predictive decision making driven by multiple time-linked reward representations in the anterior cingulate cortex. Nature communications. 2016;7:12327. doi: 10.1038/ncomms12327. PubMed PMID: 27477632; PubMed Central PMCID: PMC4974652.
31. Kolling N, Behrens T, Wittmann MK, Rushworth M. Multiple signals in anterior cingulate cortex. Current opinion in neurobiology. 2016;37:36-43. doi: 10.1016/j.conb.2015.12.007. PubMed PMID: 26774693; PubMed Central PMCID: PMC4863523.
32. Hayden BY, Pearson JM, Platt ML. Neuronal basis of sequential foraging decisions in a patchy environment. Nature neuroscience. 2011;14(7):933-9. Epub 2011/06/07. doi: 10.1038/nn.2856. PubMed PMID: 21642973; PubMed Central PMCID: PMC3553855.
33. White JK, Monosov IE. Neurons in the primate dorsal striatum signal the uncertainty of object–reward associations. Nature communications. 2016;7:12735. doi: 10.1038/ncomms12735.
34. Monosov IE, Hikosaka O. Selective and graded coding of reward uncertainty by neurons in the primate anterodorsal septal region. Nature neuroscience. 2013;16(6):756-62. Epub 2013/05/15. doi: 10.1038/nn.3398. PubMed PMID: 23666181.
35. Matsumoto M, Hikosaka O. Two types of dopamine neuron distinctly convey positive and negative motivational signals. Nature. 2009;459(7248):837-41. Epub 2009/05/19. doi: 10.1038/nature08028. PubMed PMID: 19448610; PubMed Central PMCID: PMC2739096.
36. Luk CH, Wallis JD. Choice coding in frontal cortex during stimulus-guided or action-guided decision-making. The Journal of neuroscience : the official journal of the Society for Neuroscience. 2013;33(5):1864-71. doi: 10.1523/JNEUROSCI.4920-12.2013. PubMed PMID: 23365226; PubMed Central PMCID: PMC3711610.
37. Seo H, Lee D. Temporal filtering of reward signals in the dorsal anterior cingulate cortex during a mixed-strategy game. The Journal of neuroscience : the official journal of the Society for Neuroscience. 2007;27(31):8366-77. Epub 2007/08/03. doi: 10.1523/JNEUROSCI.2369-07.2007. PubMed PMID: 17670983; PubMed Central PMCID: PMC2413179.
38. Amiez C, Joseph JP, Procyk E. Reward encoding in the monkey anterior cingulate cortex. Cerebral cortex. 2006;16(7):1040-55. doi: 10.1093/cercor/bhj046. PubMed PMID: 16207931; PubMed Central PMCID: PMC1913662.
39. Paton JJ, Belova MA, Morrison SE, Salzman CD. The primate amygdala represents the positive and negative value of visual stimuli during learning. Nature. 2006;439(7078):865-70. doi: 10.1038/nature04490. PubMed PMID: 16482160; PubMed Central PMCID: PMC2396495.
40. Klavir O, Genud-Gabai R, Paz R. Functional connectivity between amygdala and cingulate cortex for adaptive aversive learning. Neuron. 2013;80(5):1290-300. doi: 10.1016/j.neuron.2013.09.035. PubMed PMID: 24314732.

41. Takada M, Tokuno H, Hamada I, Inase M, Ito Y, Imanishi M, Hasegawa N, Akazawa T, Hatanaka N, Nambu A. Organization of inputs from cingulate motor areas to basal ganglia in macaque monkey. The European journal of neuroscience. 2001;14(10):1633-50. PubMed PMID: 11860458.
42. An X, Bandler R, Ongur D, Price JL. Prefrontal cortical projections to longitudinal columns in the midbrain periaqueductal gray in macaque monkeys. The Journal of comparative neurology. 1998;401(4):455-79. PubMed PMID: 9826273.
43. Vogt BA, Pandya DN. Cingulate cortex of the rhesus monkey: II. Cortical afferents. The Journal of comparative neurology. 1987;262(2):271-89. doi: 10.1002/cne.902620208. PubMed PMID: 3624555.
44. Haber SN, Knutson B. The reward circuit: linking primate anatomy and human imaging. Neuropsychopharmacology : official publication of the American College of Neuropsychopharmacology. 2010;35(1):4-26. doi: 10.1038/npp.2009.129. PubMed PMID: 19812543; PubMed Central PMCID: PMC3055449.
45. Haber SN, Kunishio K, Mizobuchi M, Lynd-Balta E. The orbital and medial prefrontal circuit through the primate basal ganglia. The Journal of neuroscience : the official journal of the Society for Neuroscience. 1995;15(7 Pt 1):4851-67. PubMed PMID: 7623116.
46. Ledbetter MN, Chen DC, Monosov IE. Multiple mechanisms for processing reward uncertainty in the primate basal forebrain. The Journal of neuroscience : the official journal of the Society for Neuroscience. 2016;36(30). doi: 10.1523/JNEUROSCI.1123-16.2016.
47. Monosov IE, Leopold DA, Hikosaka O. Neurons in the Primate Medial Basal Forebrain Signal Combined Information about Reward Uncertainty, Value, and Punishment Anticipation. The Journal of neuroscience : the official journal of the Society for Neuroscience. 2015;35(19):7443-59. doi: 10.1523/JNEUROSCI.0051-15.2015. PubMed PMID: 25972172; PubMed Central PMCID: PMC4429151.
48. Steimer T. The biology of fear-and anxiety-related behaviors. Dialogues in clinical neuroscience. 2002;4:231-50.
49. Craig K, Brown K, Baum A. Environmental factors in the etiology of anxiety. Psychopharmacology Raven Press, New York. 1995:1325-39.
50. Imada H, Nageishi Y. The concept of uncertainty in animal experiments using aversive stimulation. Psychological bulletin. 1982;91(3):573.
51. Grupe DW, Nitschke JB. Uncertainty and anticipation in anxiety: an integrated neurobiological and psychological perspective. Nature Reviews Neuroscience. 2013;14(7):488-501.
52. Saez A, Rigotti M, Ostojic S, Fusi S, Salzman CD. Abstract Context Representations in Primate Amygdala and Prefrontal Cortex. Neuron. 2015;87(4):869-81. doi: 10.1016/j.neuron.2015.07.024. PubMed PMID: 26291167; PubMed Central PMCID: PMC4574873.
53. Monosov IE, Hikosaka O. Regionally distinct processing of rewards and punishments by the primate ventromedial prefrontal cortex. The Journal of neuroscience : the official journal of the Society for Neuroscience. 2012;32(30):10318-30. Epub 2012/07/28. doi: 10.1523/JNEUROSCI.1801-12.2012. PubMed PMID: 22836265; PubMed Central PMCID: PMC3438659.
54. Cohen JY, Amoroso MW, Uchida N. Serotonergic neurons signal reward and punishment on multiple timescales. eLife. 2015;4. doi: 10.7554/eLife.06346. PubMed PMID: 25714923; PubMed Central PMCID: PMC4389268.

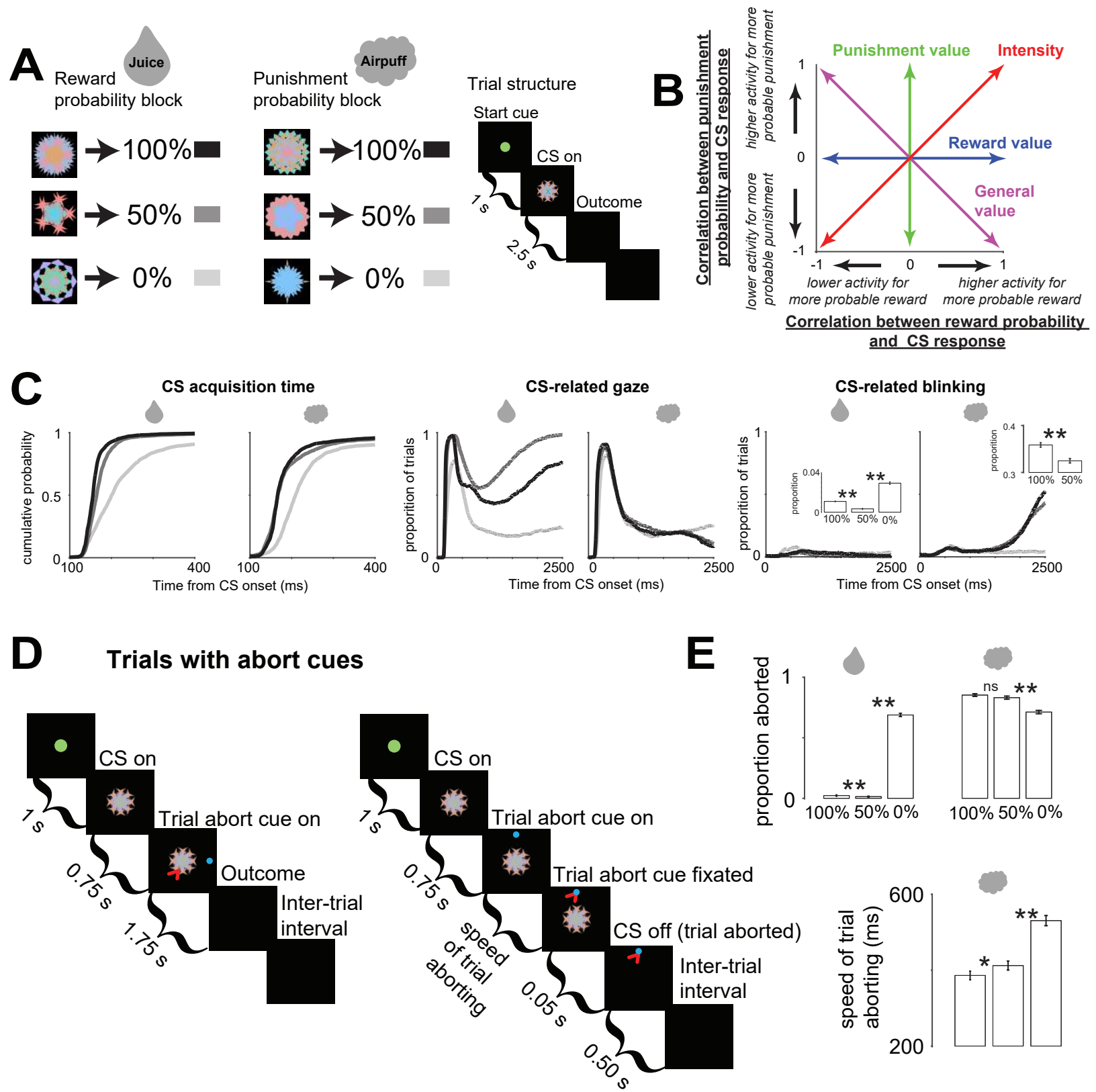
A
Reward probability block
Juice
100%
50%
0%
Punishment probability block
Airpuff
100%
50%
0%
Trial structure
Start cue
CS on
Outcome
1 s
2.5 s
B
Correlation between punishment probability and CS response
higher activity for more probable punishment
lower activity for more probable punishment
Punishment value
Intensity
Reward value
General value
lower activity for more probable reward
higher activity for more probable reward
Correlation between reward probability and CS response
C
CS acquisition time
CS-related gaze
CS-related blinking
cumulative probability
proportion of trials
Time from CS onset (ms)
D
Trials with abort cues
CS on
Trial abort cue on
Outcome
Inter-trial interval
1 s
0.75 s
1.75 s
Trial abort cue fixated
CS off (trial aborted)
speed of trial aborting
0.05 s
0.50 s
E
proportion aborted
100% 50% 0%
ns
speed of trial aborting (ms)

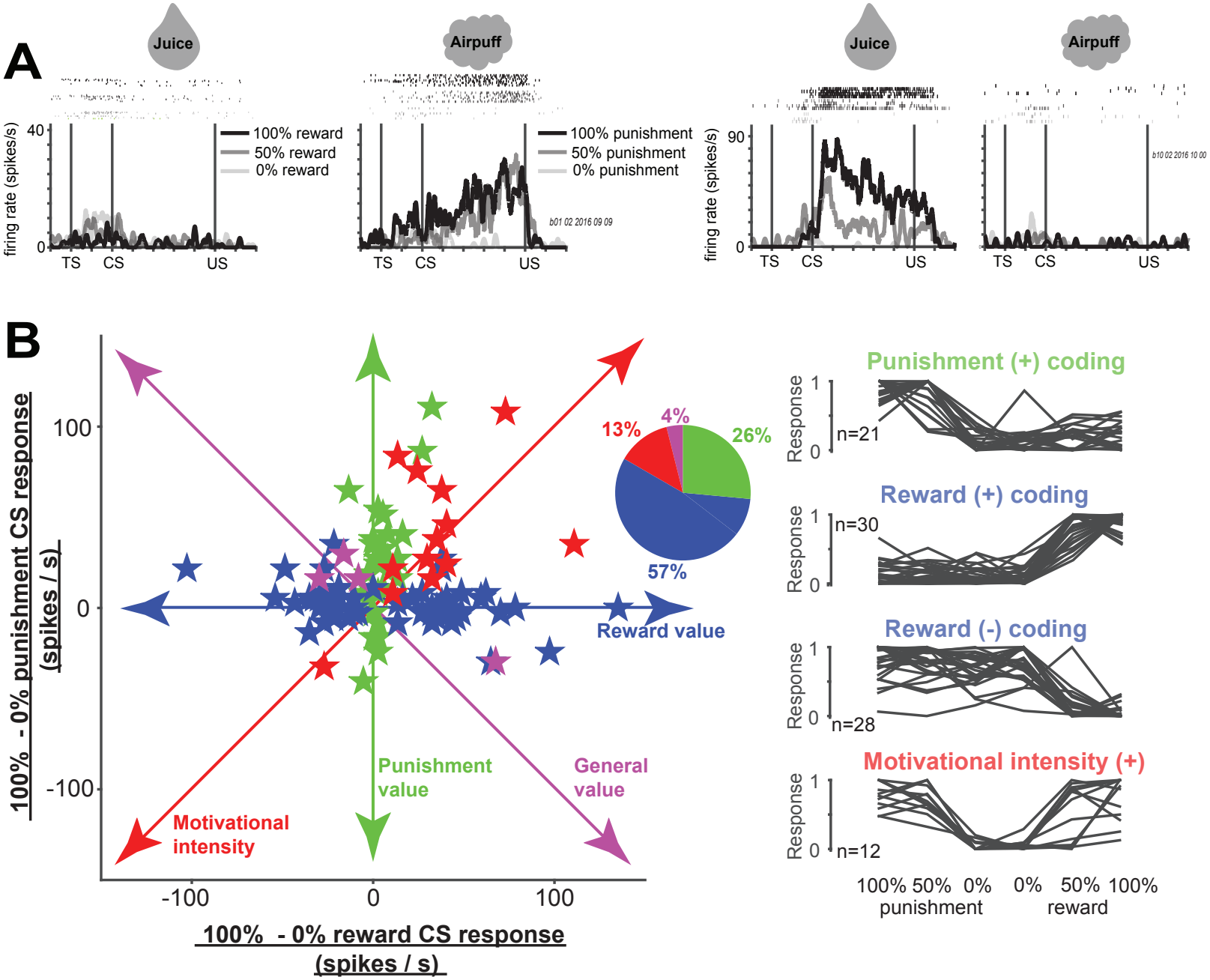
A
Juice
Airpuff
Juice
Airpuff
firing rate (spikes/s)
40
0
100% reward
50% reward
0% reward
TS
CS
US
100% punishment
50% punishment
0% punishment
b01 02 2016 09 09
90
b10 02 2016 10 00
B
100% - 0% punishment CS response
(spikes / s)
100
0
-100
100% - 0% reward CS response
(spikes / s)
Reward value
Punishment value
General value
Motivational intensity
13%
4%
26%
57%
Punishment (+) coding
Reward (+) coding
Reward (-) coding
Motivational intensity (+)
Response
n=21
n=30
n=28
n=12
100% 50% 0%
punishment
0% 50% 100%
reward

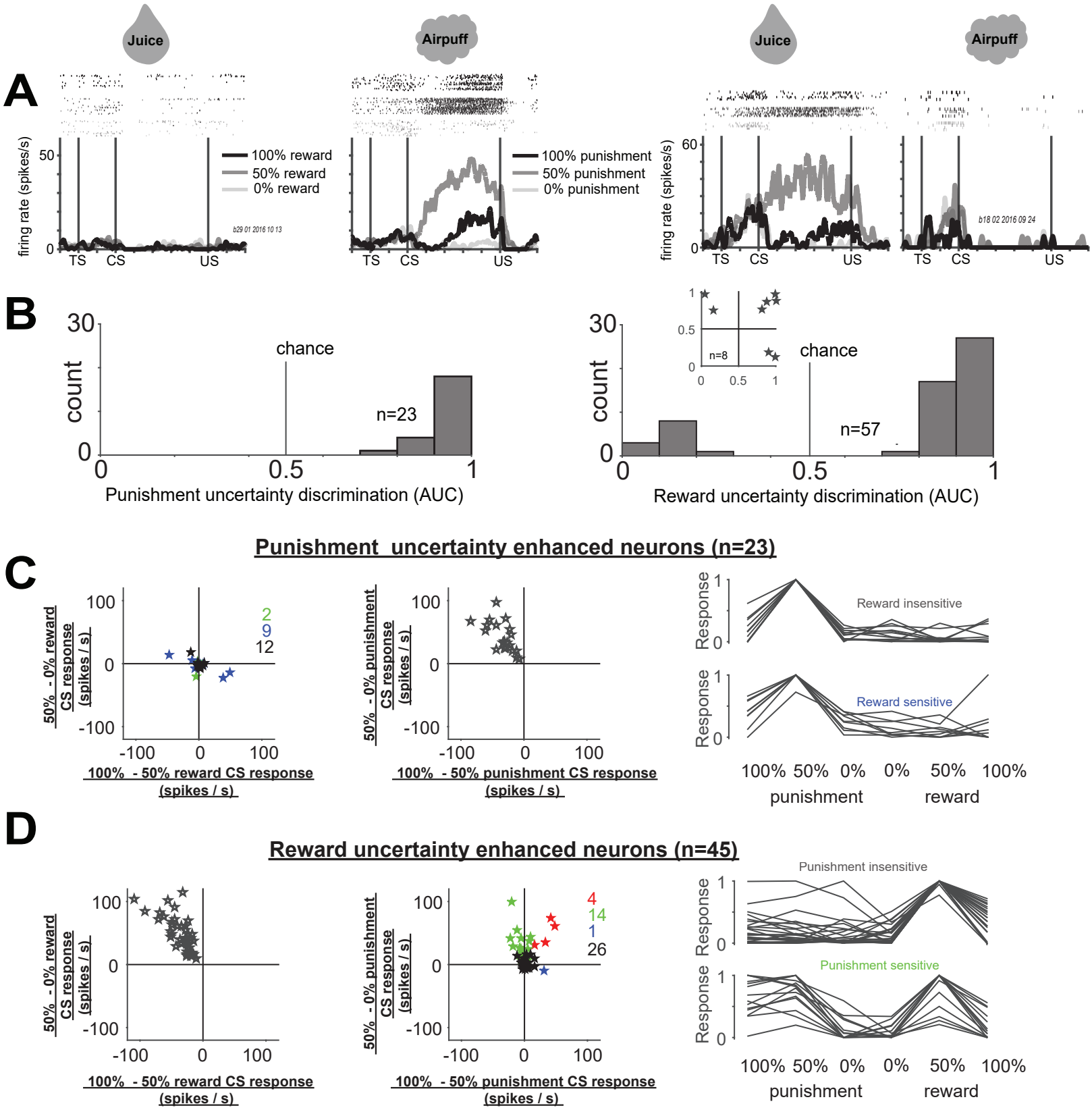
A
Juice
Airpuff
Juice
Airpuff
firing rate (spikes/s)
50
0
TS
CS
US
100% reward
50% reward
0% reward
b29 01 2016 10 13
100% punishment
50% punishment
0% punishment
60
b18 02 2016 09 24
B
count
30
0
chance
n=23
0.5
1
Punishment uncertainty discrimination (AUC)
n=8
n=57
Reward uncertainty discrimination (AUC)
C
Punishment uncertainty enhanced neurons (n=23)
50% - 0% reward CS response (spikes / s)
100
-100
2
9
12
100% - 50% reward CS response (spikes / s)
50% - 0% punishment CS response (spikes / s)
100% - 50% punishment CS response (spikes / s)
Response
Reward insensitive
Reward sensitive
100% 50% 0% 0% 50% 100%
punishment
reward
D
Reward uncertainty enhanced neurons (n=45)
4
14
1
26
Punishment insensitive
Punishment sensitive

Supplemental Figures 1 - 6

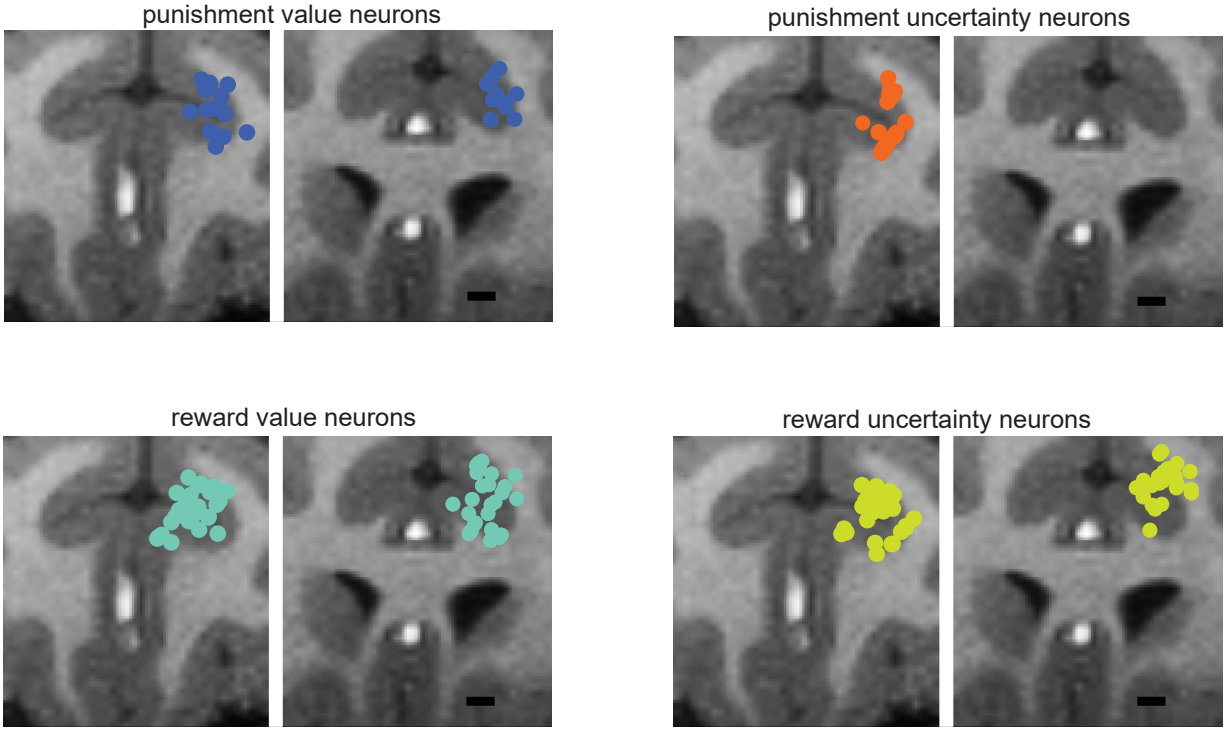
punishment value neurons
punishment uncertainty neurons
reward value neurons
reward uncertainty neurons

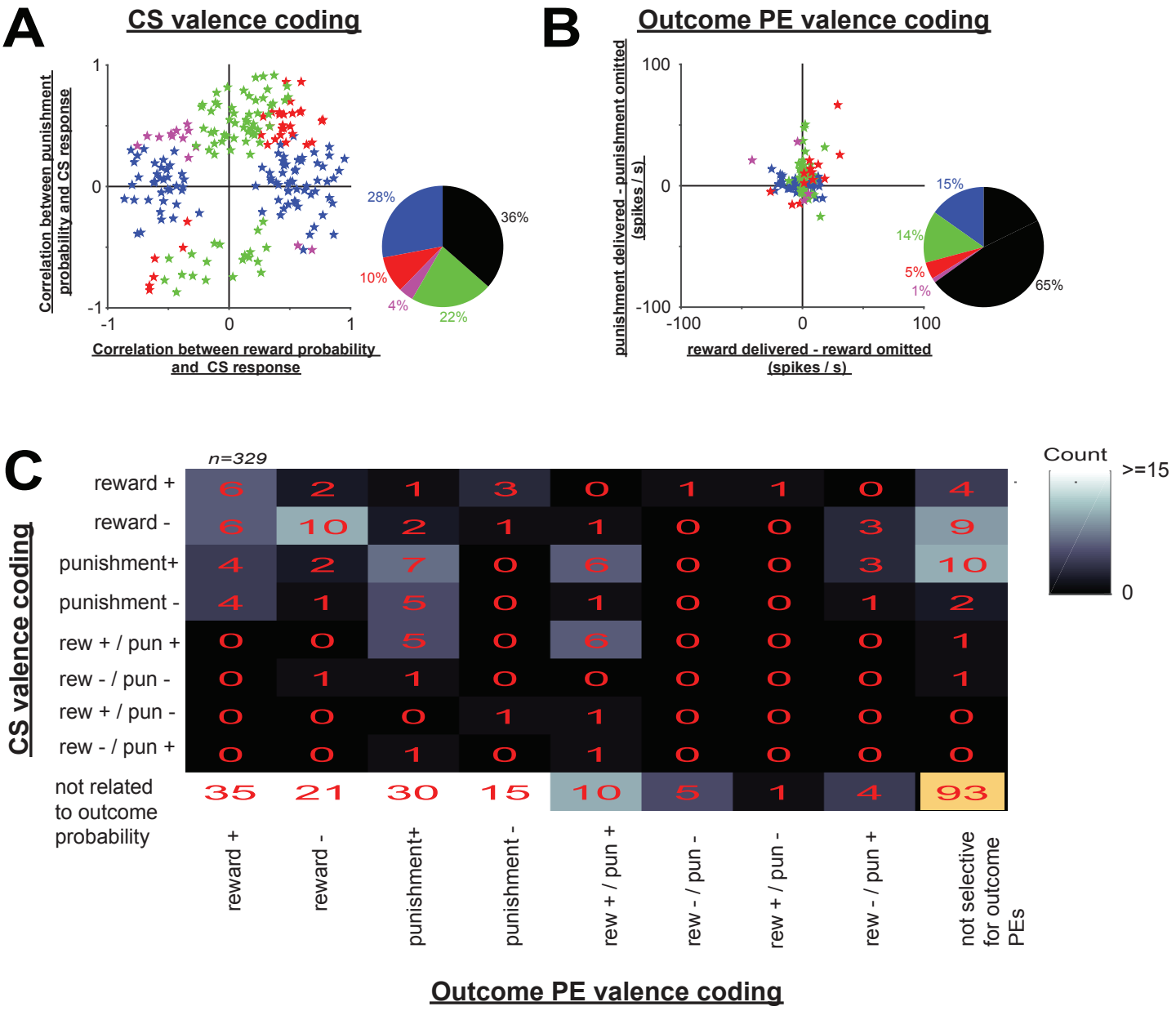
A
CS valence coding
Correlation between punishment probability and CS response
Correlation between reward probability and CS response
1
0
-1
-1
0
1
28%
36%
10%
4%
22%
B
Outcome PE valence coding
punishment delivered - punishment omitted (spikes / s)
reward delivered - reward omitted (spikes / s)
100
0
-100
-100
0
100
15%
14%
5%
1%
65%
C
n=329
CS valence coding
reward +
reward -
punishment+
punishment -
rew + / pun +
rew - / pun -
rew + / pun -
rew - / pun +
not related to outcome probability
6 2 1 3 0 1 1 0 4
6 10 2 1 1 0 0 3 9
4 2 7 0 6 0 0 3 10
4 1 5 0 1 0 0 1 2
0 0 5 0 6 0 0 0 1
0 1 1 0 0 0 0 0 1
0 0 0 1 1 0 0 0 0
0 0 1 0 1 0 0 0 0
35 21 30 15 10 5 1 4 93
reward +
reward -
punishment+
punishment -
rew + / pun +
rew - / pun -
rew + / pun -
rew - / pun +
not selective for outcome PEs
Outcome PE valence coding
Count
>=15
0

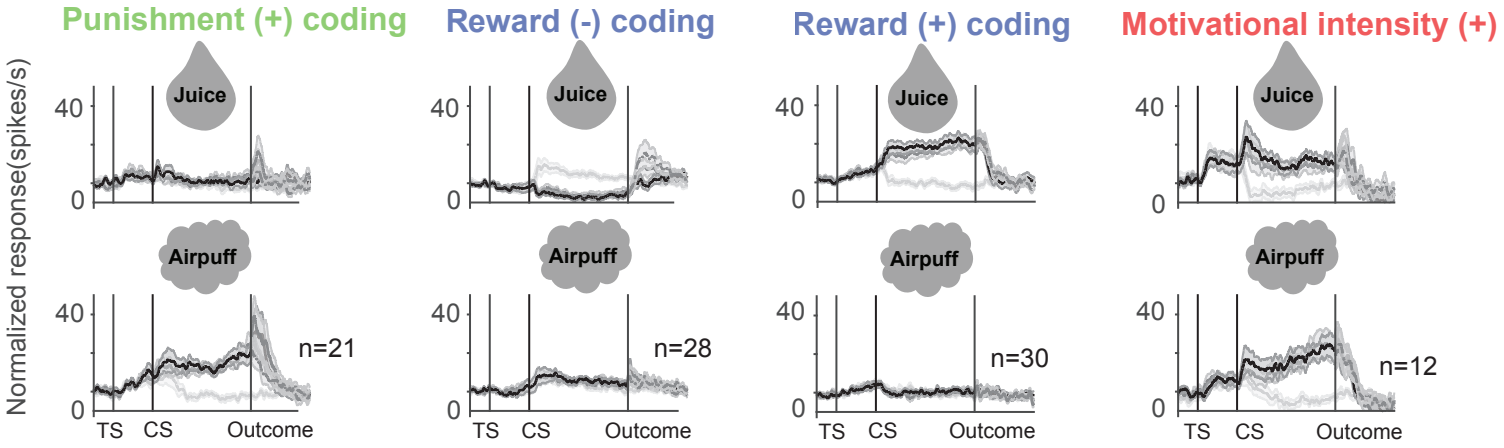
Punishment (+) coding
Reward (-) coding
Reward (+) coding
Motivational intensity (+)
Normalized response(spikes/s)
Juice
Airpuff
40
0
n=21
n=28
n=30
n=12
TS
CS
Outcome

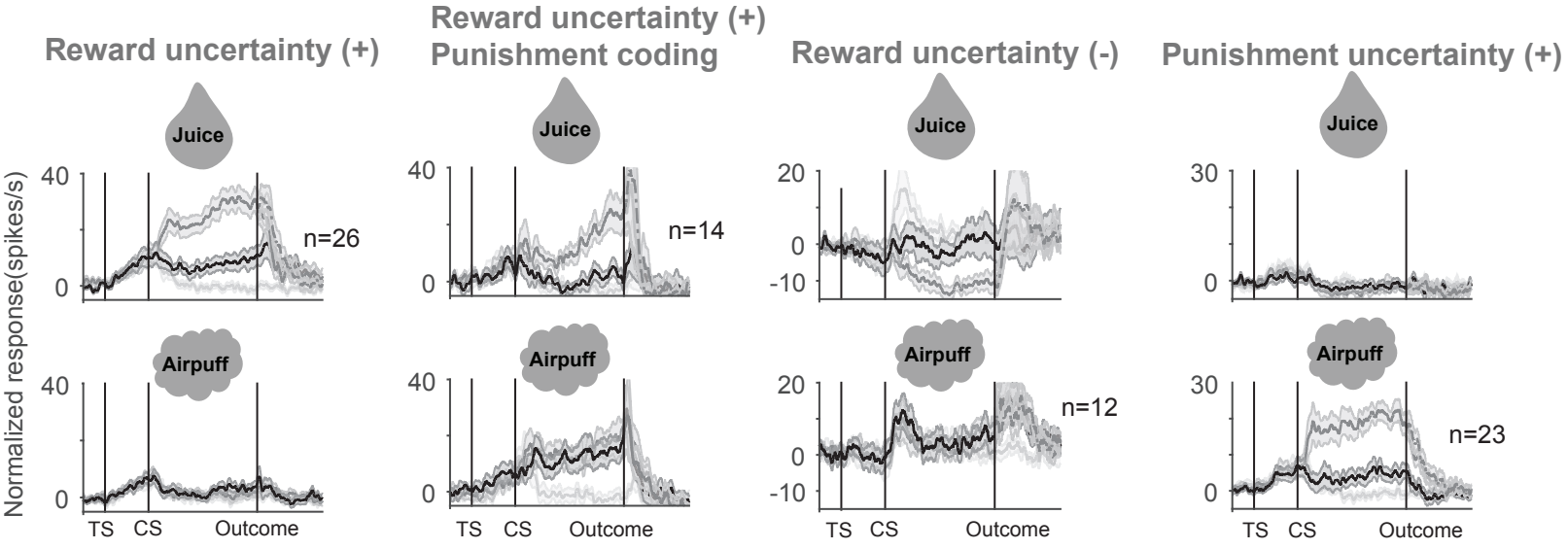
Reward uncertainty (+)
Reward uncertainty (+)
Punishment coding
Reward uncertainty (-)
Punishment uncertainty (+)
Juice
Airpuff
Normalized response(spikes/s)
40
0
20
-10
30
n=26
n=14
n=12
n=23
TS
CS
Outcome

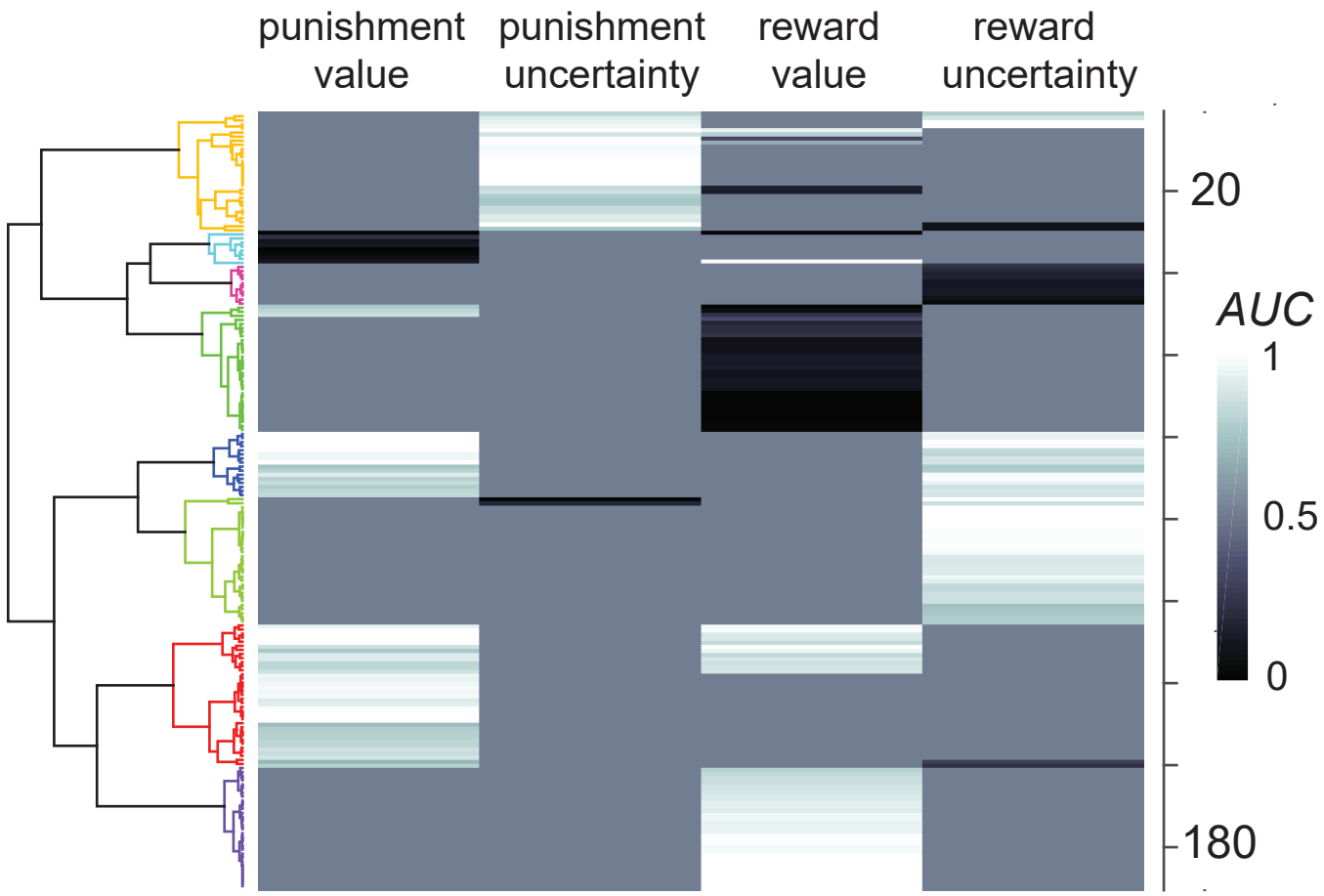
punishment value
punishment uncertainty
reward value
reward uncertainty
20
180
AUC
1
0.5
0

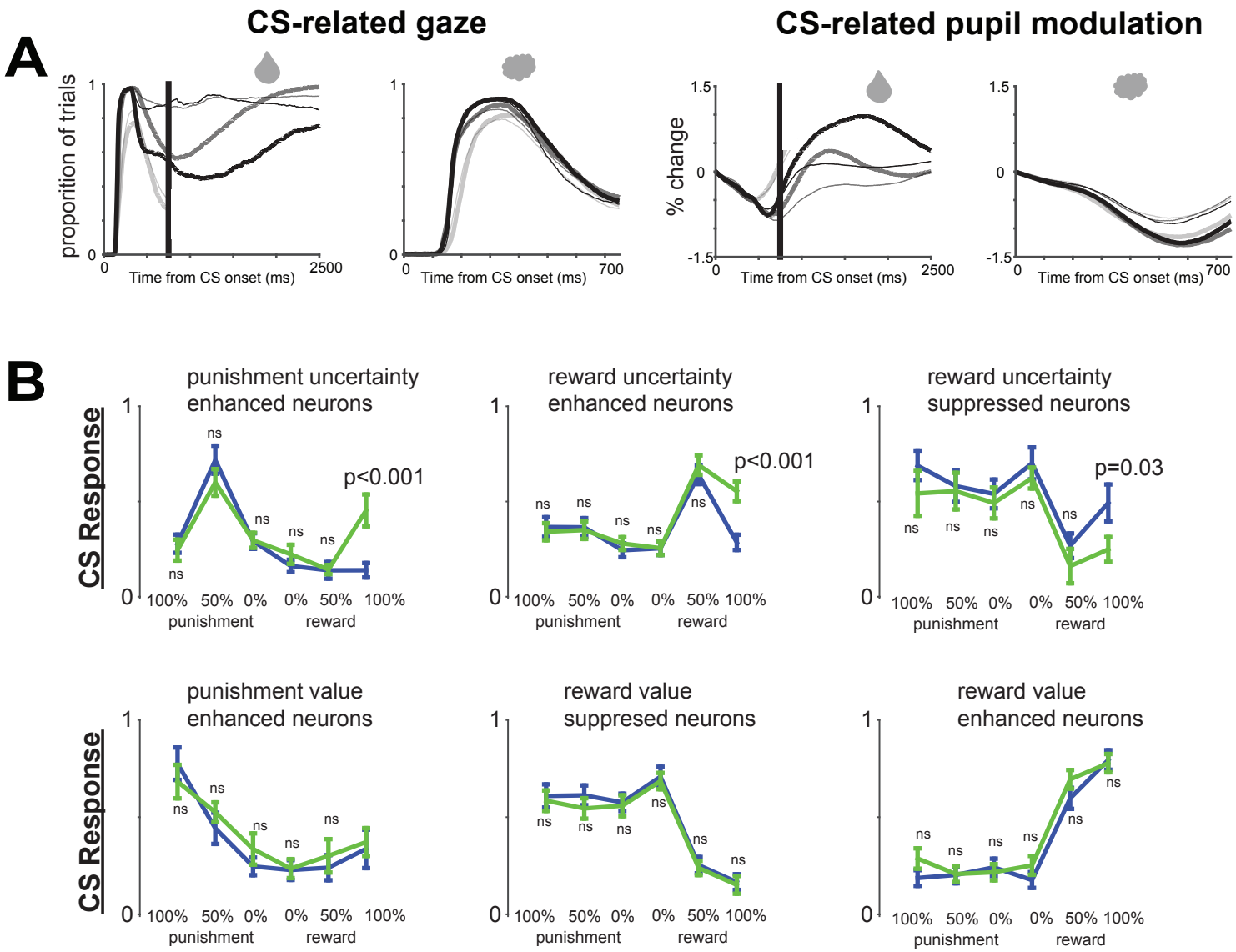
A
CS-related gaze
CS-related pupil modulation
proportion of trials
% change
Time from CS onset (ms)
B
CS Response
punishment uncertainty enhanced neurons
reward uncertainty enhanced neurons
reward uncertainty suppressed neurons
punishment value enhanced neurons
reward value suppresed neurons
reward value enhanced neurons
p<0.001
p=0.03
ns
100% 50% 0% 0% 50% 100%
punishment
reward